DIFFERENTIATION BETWEEN TOBACCO BUDWORM (*CHLORIDEA VIRESCENS*) AND BOLLWORM (*HELICOVERPA ZEA*) EGGS AT THE ORGANISMAL LEVEL: NEW PERSPECTIVES

Roger D. Lawrie
Kaiying Chen
Jean Marcel Deguenon
Loganathan Ponnusamy
DeShae Dillard
Daniela T Pezzini
Hayden Schug
Dominic Reisig
Nithin M. Ganji
Hannah Burrack
Batool Karim-Delavar
Coby Schal
Rick Santangelo
Matthew Bertone
R. Michael Roe
NC State University
Raleigh, NC
Ryan W Kurtz
Cotton Incorporated
Cary, NC

Abstract

Two lepidopteran species, tobacco budworm, *Chloridea virescens*, and bollworm, *Helicoverpa zea*, are important pests of cotton agriculture in the United States. Pest management strategies for these species require different approaches. One major difference is that bollworm requires a higher dose for many commercialized Bt proteins and is evolving field resistance to Bt-transgenic crops in comparison to the budworm. In order to improve species identification for these caterpillars at the egg stage, which could improve foliar insecticide spray recommendations, we examined potential novel techniques to differentiate between species. Eggs were analyzed using Raman spectroscopy to characterize the surface chemical components, UV fluorescence and scanning light spectroscopy to determine differences in fluorescence or color, and digital, modern photography to visualize morphological differences. No fluorescence or color differences were found between bollworm and budworm eggs for caterpillars reared on artificial diet but additional opportunities were presented from this research. Differences in surface chemistry suggest the potential for using differential staining in species diagnostics. The potential was also established for a rapid and automated field diagnosis of species using modern approaches in digital photography and machine learning, to detect egg morphological differences with hand held cameras or even smart phones.

Introduction

Tobacco budworm, *Chloridea virescens*, and bollworm, *Helicoverpa zea*, (both species are in the Lepidoptera order and Noctuidae family) are both economically important agricultural pest species prevalent in the United States (Zeng et al., 1998). These species feed on a wide variety of different agricultural products including corn, cotton, tobacco, soybeans, wheat, and household gardens (University of Florida, 2018; USDA 1925). Integrated pest management practices (IPM) for caterpillar control include the use Bt-transgenic crops expressing insecticidal proteins augmented as needed with chemical insecticide sprays, e.g., pyrethroids and others. Unfortunately, resistance to these tactics has become widespread in varying degrees (Plapp et al., 1990; Luttrell et al., 1998; Zeng et al., 1998). Most importantly, *H. zea* requires a higher dose for many commercialized Bt proteins and is evolving resistance to Bt-transgenic crops in comparison to *C. virescens* (Lawrie et al., 2020 and papers cited therein). Oftentimes to control *H. zea*, sprayable insecticides must be used in addition to the Bt protein toxins produced by GMO crops (Reisig et al., 2019; University of California, 2020).

The most crucial step for pest management is correct identification of the pest species; this allows for the application of the appropriate management technique for that particular insect (EPA 2020) and whether in addition to GMO crops engineered for caterpillar control, chemical sprays are needed (University of California, 2020 A,B). Before the

evolution of field Bt resistance in *H. zea*, cotton thresholds for *C. virescens* and *H. zea* were based on either the presence of live larvae or damaged reproductive tissue (Del Pozo-Valdivia et al. In press). However, once *H. zea* evolved resistance, these thresholds allowed unacceptable injury and larval control using foliar insecticides was difficult. As a result, egg-based thresholds were adopted (Reisig et al. 2019).

Chloridea virescens and *Helicoverpa zea* are difficult to differentiate at the egg stage and early instars (Zeng et al., 1998). Differentiation of these species is important, since *C. virescens* is still susceptible to all commercially available Bt cotton cultivars (Reisig et al. 2019). Hence, foliar insecticide sprays could be triggered based on the presence of *C. virescens* eggs, circumventing the effectiveness Bt cotton and causing unneeded sprays. Currently, the predominant means of species identification of eggs are reliant on morphology, which requires extensive training or expensive equipment and even electron microscopy (Zeng et al., 1998). Morphological similarities between the two species include a white to gray color, round shape, and high ridges (Zeng et al., 1998). Morphological differences are predominantly in the micropyle region of the egg where the primary ribs terminate before touching the rosette in *C. virescens* while in *H. zea* the ribs continue to the rosette. Additionally, there are cross ribs present in *H. zea* that are absent in *C. virescens*. Also in *C. virescens*, there is punctuation present on the egg surface which is absent in *H. zea* (Zeng et al., 1998). These differences are difficult to see and are most apparent by scanning electron microscopy (Zeng et al., 1998). Additionally, monoclonal antibodies have been used to identify egg species (Hagler et al., 1991; Trowell et al., 1993; Greenstone et al., 1995). This method was commercialized at one time into an antibody test kit by Agdia, Inc. While species-specific antibodies have been used to differentiate between *H. zea* and *C. virescens*, this identification technique is not always accurate (Zeng et al., 1998). There are other challenges with an antibody approach including a limited shelf life of kits, cost per assay, and ease of using the kits in the field. Expansion of identification methods of *H. zea* and *C. virescens* at the egg stage will aide in selection of optimal IPM approaches which will in turn reduce economic and environmental costs of pest control. If a grower can determine species at the egg level, they can make early decisions on whether or not insecticide application is required.

The objectives of this study were to expand upon current species identification techniques for *H. zea* and *C. virescens* and in so doing, develop ideas on better field diagnosis and which could be expanded to other caterpillar species and insects in general. We examined the following approaches: (*i*) egg surface chemistry using Raman spectroscopy to assess the potential of using differential staining of the egg for species diagnosis; (*ii*) UV fluorescence and light scanning differences between species; and (*iii*) compound light microscopy and photography with camera attachments to determine whether modern imaging equipment is able to visualize morphological differences between egg species.

Materials and Methods

Egg Acquisition

Helicoverpa zea pupa were acquired from a laboratory colony raised on artificial diet. *Chloridea virescens* pupa were acquired from another lab colony at NCSU reared on artificial diet. Pupa were allowed to emerge in separate growth chambers at 14:10 L:D, 27 °C, and 60% RH. Moths for each species were transferred to ovipositional chambers consisting of a plastic bucket with the opening covered with cheesecloth. Once emerged, adults were given a 10% sucrose solution *ad libitum* using a wick system. Eggs oviposited on the cheese cloth were collected and stored at -40 °C at the following ages after oviposition: 0 h, 12 h, 24 h, 36 h, and 48 h. Gloves were used in handling the eggs in order to prevent contamination.

Raman Spectroscopy

The NC State Analytical Instruments Facility (AIF) performed Raman Spectroscopy for this project to examine differences in the egg surface components between species. For these experiments, live eggs were used for both species within 48 h of oviposition. Four different locations surrounding the micropyle region were targeted for analysis for each species of egg. One egg was used for each species. The Raman spectrometer used for this analysis was a Horiba XploRA ONE (Horiba Jobin Yvon Inc., Edison, NJ, USA) with a 532 nm laser and a CCD detector. The analysis was performed with a 25% laser intensity (25 mW at full power) with a 3 s acquisition time and 3 accumulations per location. The grating used was 1200 (750 nm) groom density with hole and slit measurements of 500 and 200 µm, respectively, for each location. The ICS correction was also on for these experiments. Four different locations were analyzed on each species of egg. All predicted functional group assignments were made using the Horiba Raman Data and Analysis handbook (Horiba Jobin Yvon Inc., Edison, NJ, USA).

UV Fluorescence

In order to analyze differences in fluorescence between species, UV fluorescence imaging was performed using a Benchtop UVP UV transilluminator (312 nm) (ThermoFischer Scientific, Waltham, Massachusetts, USA). Eggs that were frozen at 0 h for both species were examined. Eggs oviposited on cheesecloth were frozen until needed for study and applied to the transilluminator directly. Photographs of any fluorescence were taken using a mobile phone camera.

Scanning Spectroscopy

A scanning spectrophotometer was used to analyze any differences in absorbance of each species of egg. Scanning spectrophotometry is a useful tool in analyzing absorbance properties related to color, and this technique was used to compare differences between caterpillar species for different aged eggs. For each trial, 50 eggs were mechanically homogenized in 200 µL of DI H_2O and then then centrifuged at 1.0 g for 10 min at room temperature. Into each well, 55 µL of supernatant was added, and a wavelength scan conducted using a SpectraMax Plus 384 plate reader (Molecular Devices, San Jose, CA, USA) using the SoftMax Pro program (Version 7.1). Absorbance was measured from 350 to 750 nm at room temperature. A total of 9 trials for each species was performed following this protocol. For control (blank) measurements, 55 µL of DI H_20 was used.

Compound Light Microscopy and Camera Attachment Photography

In order to determine the efficacy of modern microscopy and photography equipment in visualizing the morphological differences between *H. zea* and *C. virescens*, egg photographs were taken with two different types of imaging equipment. First a compound light microscope (Leitz LaborLux II) and Amscope 1080p digital microscope camera was used to image eggs for both *H. zea* and *C. virescens.* The AmScope program (v. 3.7) was used to take photographs; pictures were taken via the ocular lens of the compound light microscope. Magnifications of 10x for the ocular lens with 4x and 10x for the objective lens were used. Images were stacked using 8 image layers for z-stacking with the ImageJ software. Secondly, photographs were taken with a portable camera with a microscope objective lens attached. Images were taken using a Canon 60D DSLR equipped with a 20X microscope objective attached to the camera using extension tubes. The camera was mounted to a Cognisys Stackshot Macro Rail for automated z-stacking of the eggs. Forty-five image layers were taken of each egg and processed into a single image using Zerene Stacker software (http://zerenesystems.com/cms/stacker). Eggs used for these photographs were preserved in a -40 ºC freezer prior to photography.

Figure Construction

Figures and tables for this paper were constructed using Microsoft Excel and PowerPoint (2018).

Results and Discussion

Raman Spectroscopy

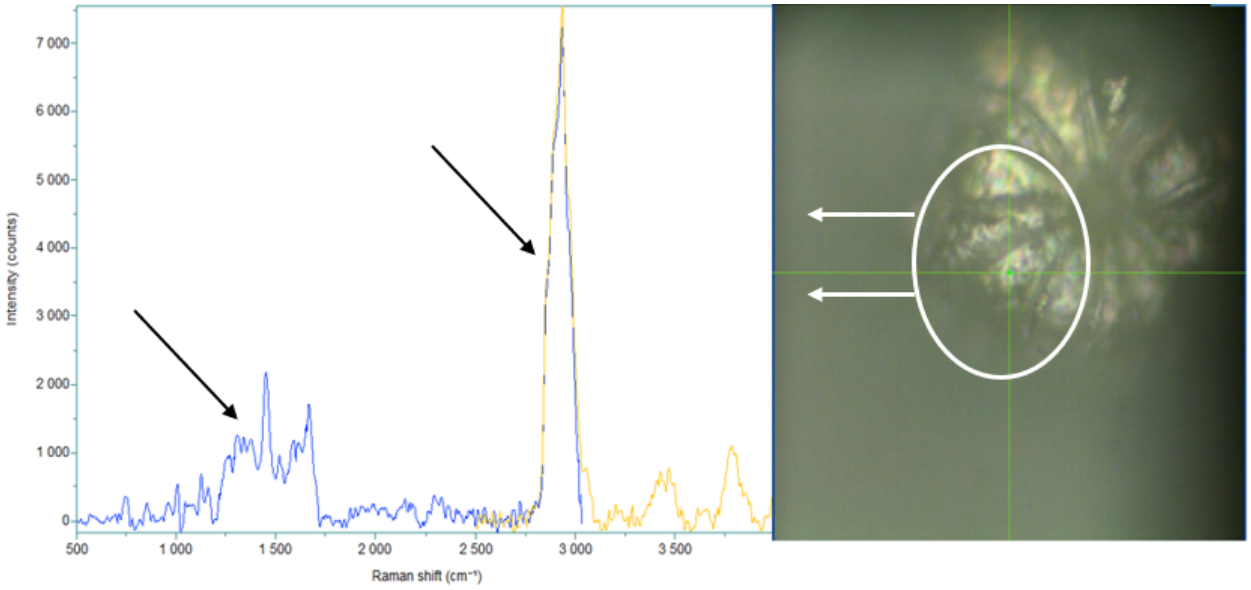

Figure 1. Raman spectroscopy for the *Chloridea virescens* egg surface (rosette region), location 1. The image to the right is the location targeted for analysis on the egg surface, indicated by the green cross-hairs inside of the white circle. The graph to the left is the resulting spectroscopy data. Major peaks are indicated by black arrows. The x-axis indicated the Raman shift (cm^{-1}) and the y-axis indicates the intensity (number of counts). These data indicated by the arrows were used to assign potential functional groups to the egg surface.

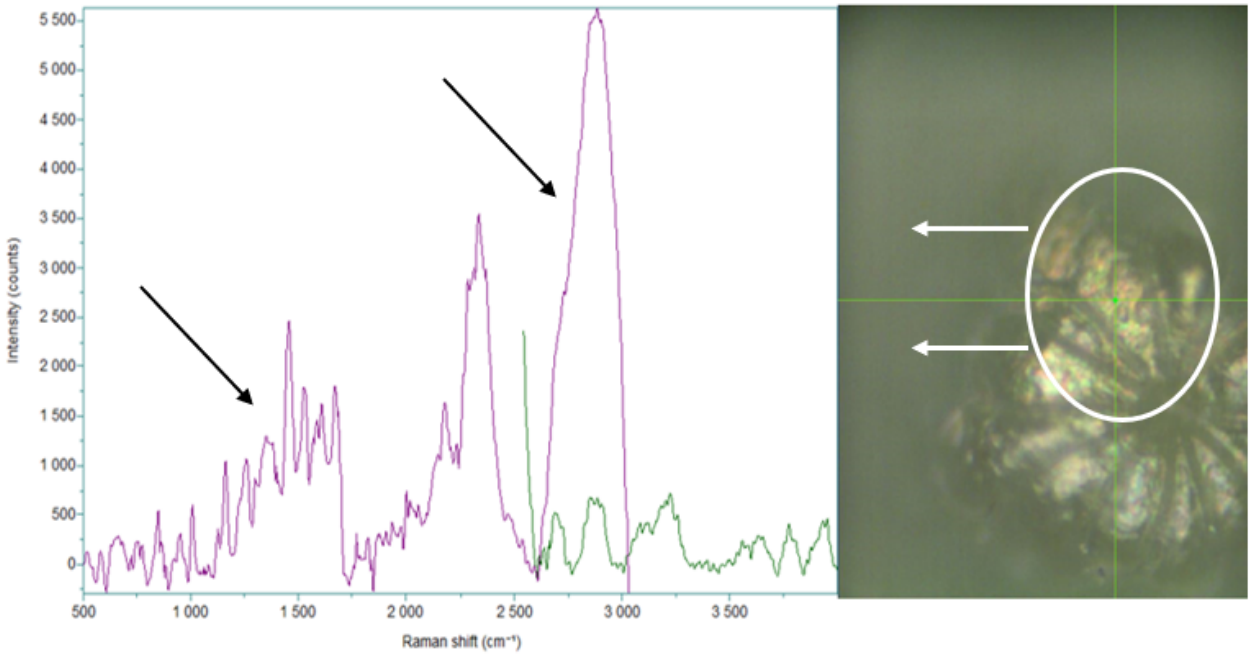

Figure 2. Raman spectroscopy for *Chloridea virescens* egg surface (rosette region), location 2. The image to the right is the location targeted for analysis on the egg surface, indicated by the green cross-hairs inside of the white circle. The graph to the left is the resulting spectroscopy data. Major peaks are indicated by black arrows. The x-axis indicated the Raman shift (cm^{-1}) and the y-axis indicates the intensity (number of counts). These data indicated by the arrows were used to assign potential functional groups to the egg surface.

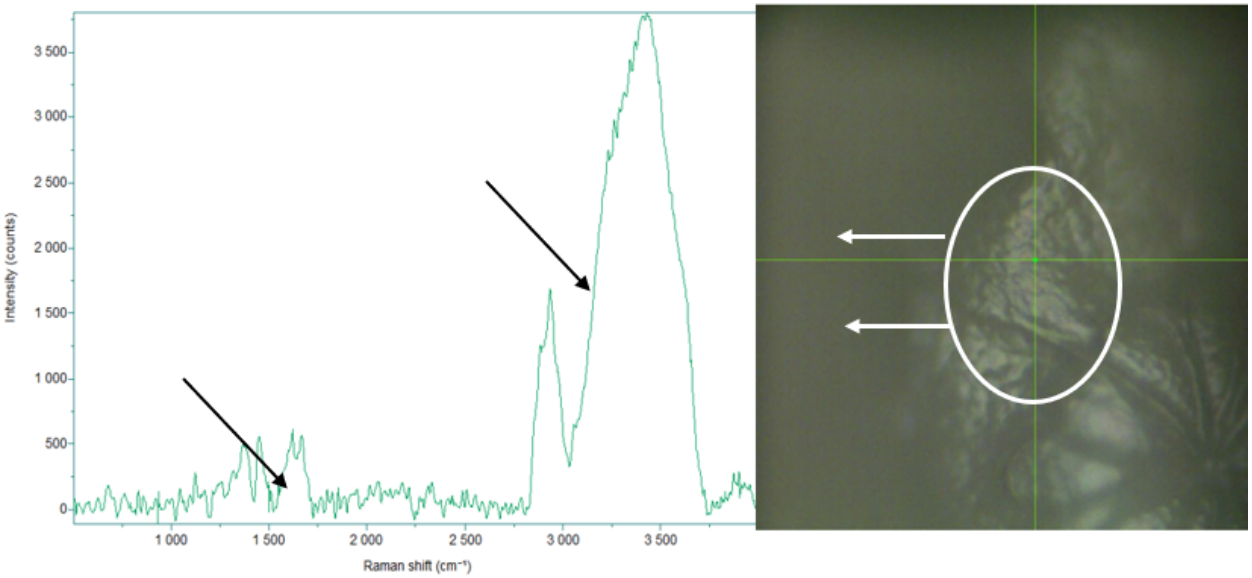

Figure 3. Raman spectroscopy for *Helicoverpa zea* egg surface (rosette region), location 1. The image to the right is the location targeted for analysis on the egg surface, indicated by the green cross-hairs inside of the white circle. The graph to the left is the resulting spectroscopy data. Major peaks are indicated by black arrows. The x-axis indicated the Raman shift (cm^{-1}) and the y-axis indicates the intensity (number of counts). These data indicated by the arrows were used to assign potential functional groups to the egg surface.

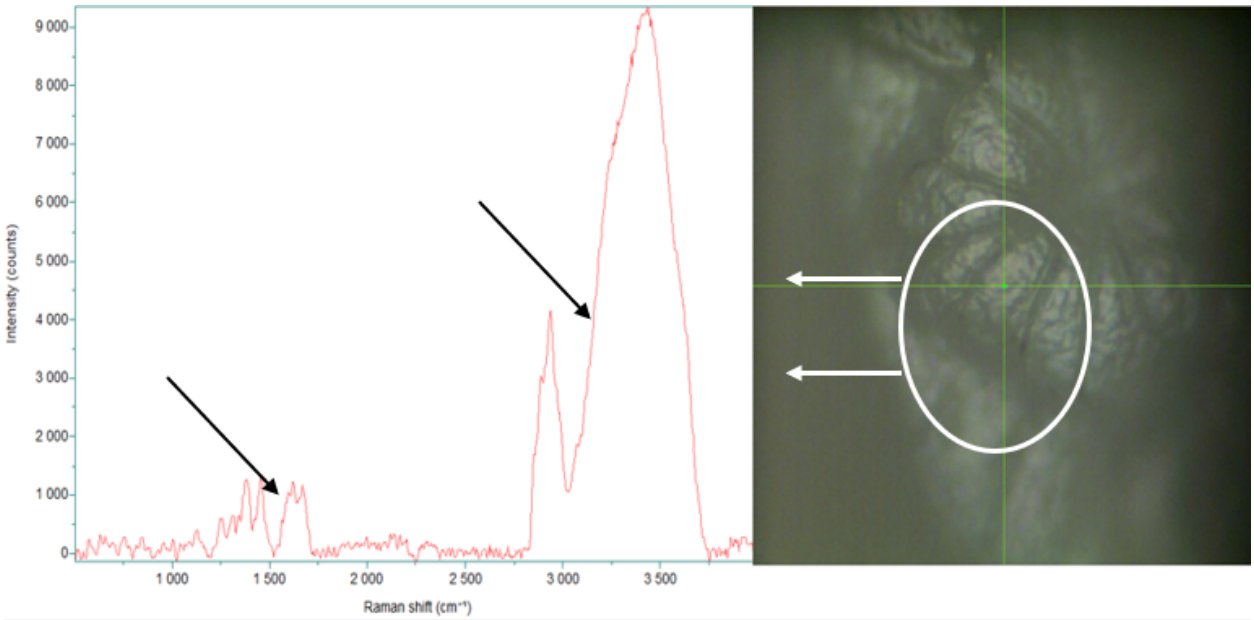

Figure 4. Raman spectroscopy for *Helicoverpa zea* egg surface (rosette region), location 2. The image to the right is the location targeted for analysis on the egg surface, indicated by the green cross-hairs inside of the white circle. The graph to the left is the resulting spectroscopy data. Major peaks are indicated by black arrows. The x-axis indicated the Raman shift (cm^{-1}) and the y-axis indicates the intensity (number of counts). These data indicated by the arrows were used to assign potential functional groups to the egg surface.

Fig. 1 depicts the Raman shifts for the first location in *Chloridea virescens* eggs. This first location is located on the rosette area of the egg (indicated by the green cross hairs). Predicted peaks and assignments in this figure are as follows: a weak peak at 1060-1150 cm^{-1} which could indicate a C-O-C asymmetrical bond, a medium peak at 1450 cm^{-1} which could indicate C-C aromatic ring chain vibrations, and a strong peak at 2800-3000 cm^{-1} which could indicate a C-H bond (Fig. 1). Fig. 2 depicts the Raman Shift data for the second location on *Chloridea virescens* eggs. This location was also on the rosette area of the egg. The predicted peak and functional group assignments are as follows: a strong peak at 2600-3000 cm^{-1} which could indicate a C-H bond, a medium/strong peak at 2300-2450 cm^{-1} which did not have any specific assignments in the Horiba manual, and a medium peak at 1450 cm^{-1} which could indicate C-C aromatic ring vibrations (Fig. 2). Fig. 3 depicts the Raman Shift data for the first location on *Helicoverpa zea* eggs. This location is just outside of the rosette region on the egg (indicated by the green cross hairs). Major potential peak and functional group assignments are as follows: a weak/broad peak at ~1640 cm^{-1} which could indicate an H_20, a medium peak at 2850-3000 cm^{-1} which could indicate a C-H bond, and a strong peak at 3050- 3650 cm^{-1} which did not have any specific assignments in the Horiba manual (Fig. 3). Fig. 4 depicts the Raman Shift data for the second location on *Helicoverpa zea* eggs. This location was on the rosette region of the egg. The major potential peak and functional group assignments were as follows: a weak/broad peak at ~1640 cm^{-1} which could indicate a H_20, a medium peak at 2850-3000 cm^{-1} which could indicate a C-H bond, and a strong/broad peak at 3050-3650 cm^{-1} which did not have any specific assignments in the Horiba manual (Fig. 4). Overall, there were two major differences in Raman shifts. For *C. virescens*, for both locations there was a strong peak at ~2600-3000 cm-1 which was not present in either *H. zea* trial (Figs. 1-4). For *H. zea*, for both locations there was a strong peak at ~2800-3750 cm^{-1} which was not present in either *C. virescens* (Figs. 1-4).

We were able to successfully identify differences in the surface chemical components of the two egg species. The presence of unique peaks was found in both trials for both species of egg (Figs. 1-4). More data are required to fully characterize the surface chemical components of the different species. In the near future, we will be performing two other techniques, Time of Flight Mass Spectrometry and GC-Mass Spectrometry, to expand on the characterization of egg surface components (work in process). Once the surface chemical components of both egg species are established, this information will be used to assess the potential use of differential staining in species diagnosis.

UV Fluorescence

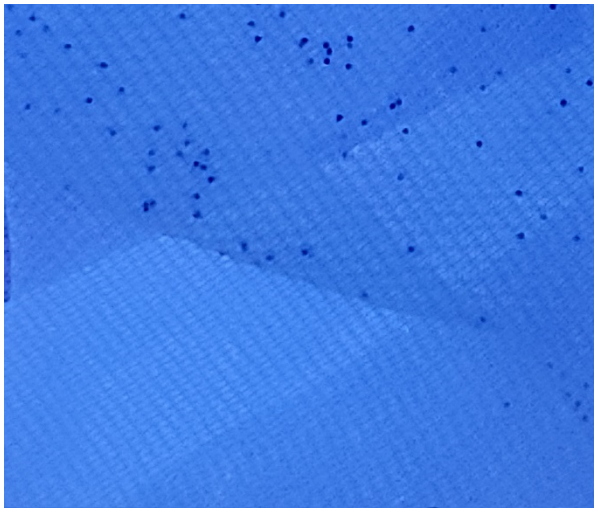

Figure 5. Frozen *Chloridea virescens* eggs oviposited on cheesecloth and placed on a UV light transilluminator (312nm).

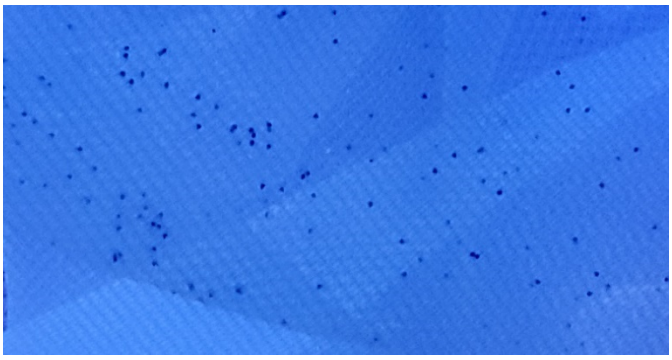

Figure 6. Frozen *Helicoverpa zea* eggs oviposited on cheesecloth and placed on a UV light transilluminator (312nm).

We examined frozen (at age 0h) eggs of both species under a UV-spectrum transilluminator at 312 nm. This was done in order to determine if these caterpillar eggs demonstrated fluoresce under UV light. Fig. 5 and 6 depict both species of egg on the UV-spectrum transilluminator. There was no observable fluorescence for either species using this wavelength of UV light (Figs. 5-6).

The experiments assessing fluorescence of *C. virescens* and *H. zea* eggs did not show any visible fluorescence at the wavelength tested (312 nm) (Fig. 5-6). However, it is possible that at other wavelengths of light within the UV spectrum (which is 10-400 nm) might produce fluorescence. The two species of eggs were examined for UV fluorescence since this technique has been used before for arthropod identifications where morphology is challenging (Kumlert et al., 2018). If fluorescence at other specific wavelengths can be established for either of these species of egg, it would be simple to develop a tool that used that particular wavelength of UV to identify the species of eggs in the field.

Scanning Spectroscopy

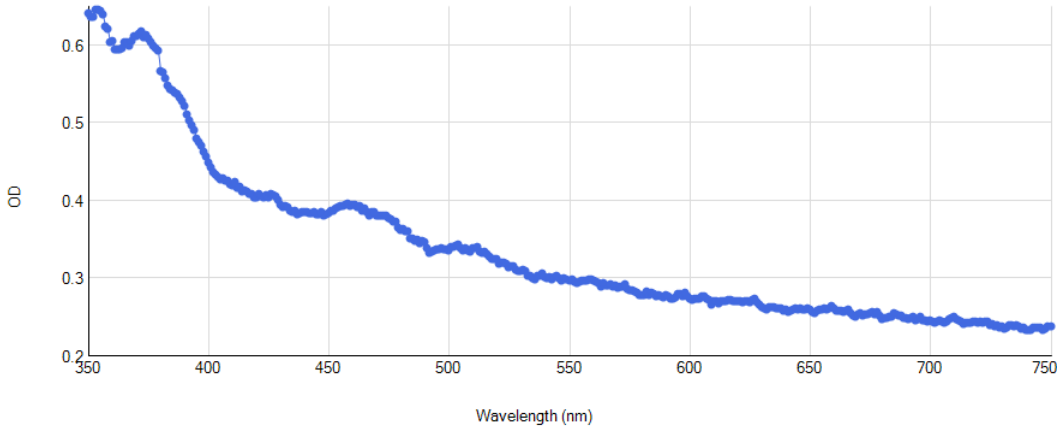

Figure 7. *Helicoverpa zea* scanning absorption spectrum, trial 1. The Y-axis depicts absorbance at each wavelength of light tested (X-axis is wavelength in nm). The wavelengths ranged from 350-750 nm.

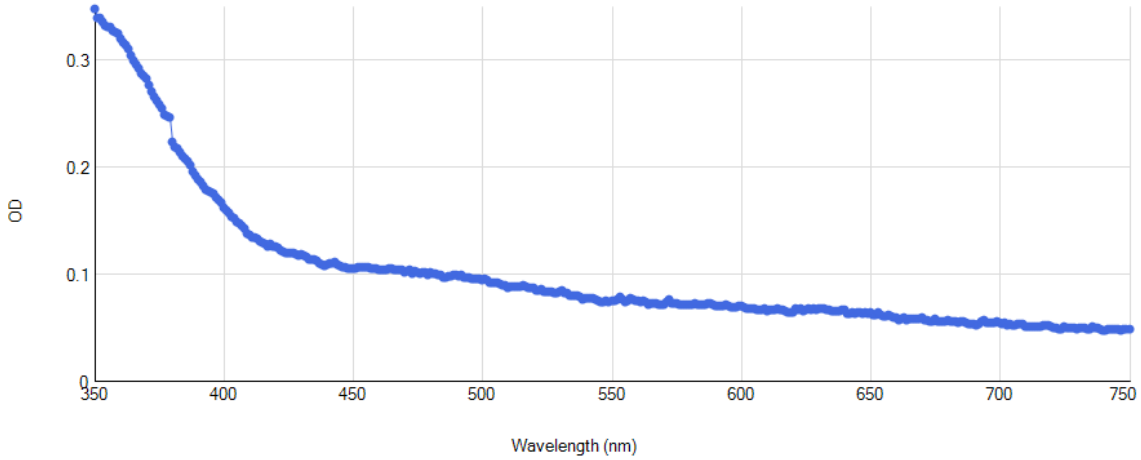

Figure 8. *Helicoverpa zea* scanning absorption spectrum, trial 2. The Y-axis depicts absorbance at each wavelength of light tested (X-axis is wavelength in nm). The wavelengths ranged from 350-750 nm.

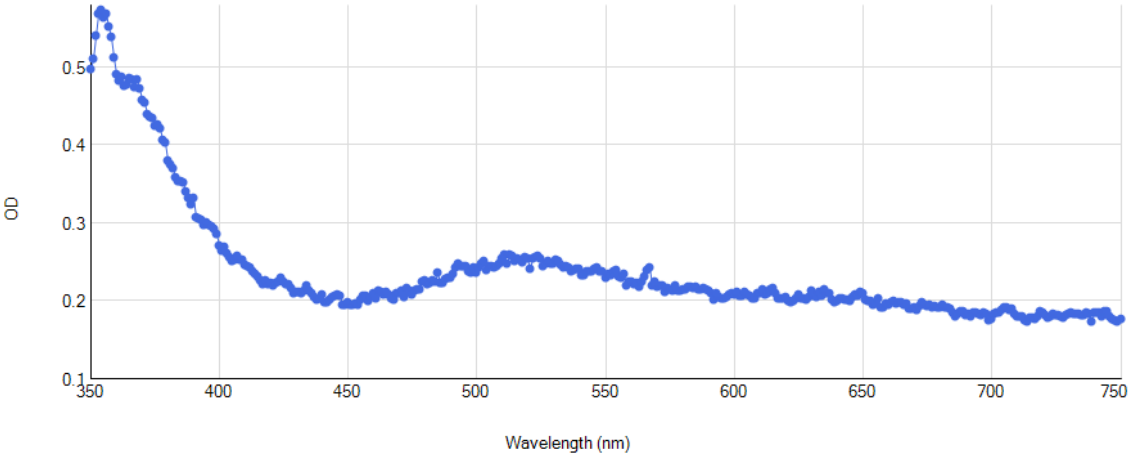

Figure 9. *Chloridea virescens* scanning absorption spectrum, trial 1. The Y-axis depicts absorbance at each wavelength of light tested (X-axis is wavelength in nm). The wavelengths ranged from 350-750 nm.

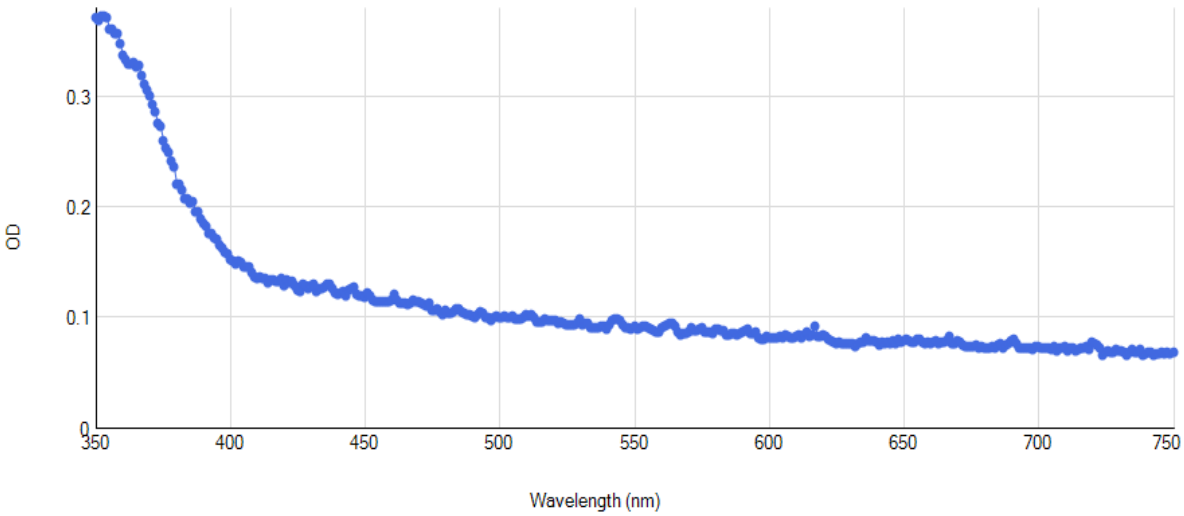

Figure 10. *Chloridea virescens* scanning absorption spectrum, trial 2. The Y-axis depicts absorbance at each wavelength of light tested (X-axis is wavelength in nm). The wavelengths ranged from 350-750 nm.

In order to assess possible differences in color between species, scanning spectroscopy experiments were conducted. We performed 10 trials for each species. For *H. zea*, one trial showed a peak at 375 nm, however this same pattern was not present in other trials for *H. zea* (Figs. 7-8). For *C. virescens*, one trial showed a peak at 360 nm, however this same pattern was not present in other trials for *C. virescens* (Figs. 9-10).

The scanning spectroscopy results for these experiments indicate that there were no consistent, significant differences in absorbance between the two species of eggs after conducting 10 trials for each species (Figs. 7-10). These insects were reared on artificial diet and the results showed no differences. It is possible, however, that field-collected eggs may have differences in absorbance because of differences in food preference and/or environmental factors. More detailed work is also needed to look at the impact of egg age on color and species diagnosis.

Egg Photography

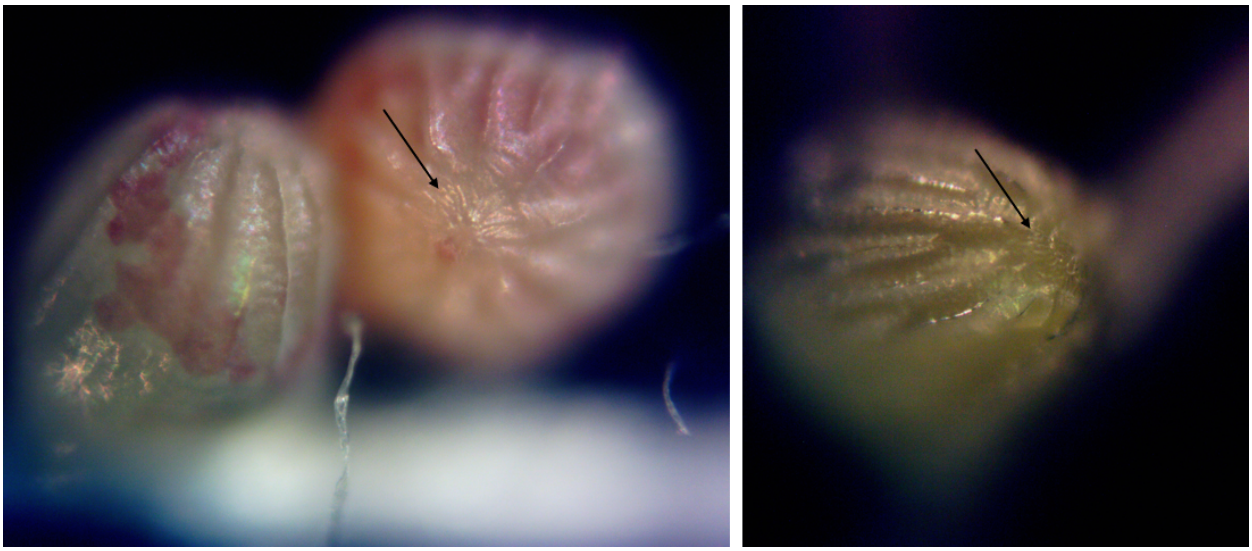

Figure 11. *Chloridea virescens* eggs, (10X objective lens) photographs taken with a compound light microscope and AmScope attachment. Photo to the left is focused directly on the rosette area of the egg. Photo to the right is focused on the rosette area from an angle. Black arrows indicate the location of expected diagnostic morphological features (primary ribs not extending to rosette and cross-ribs absent).

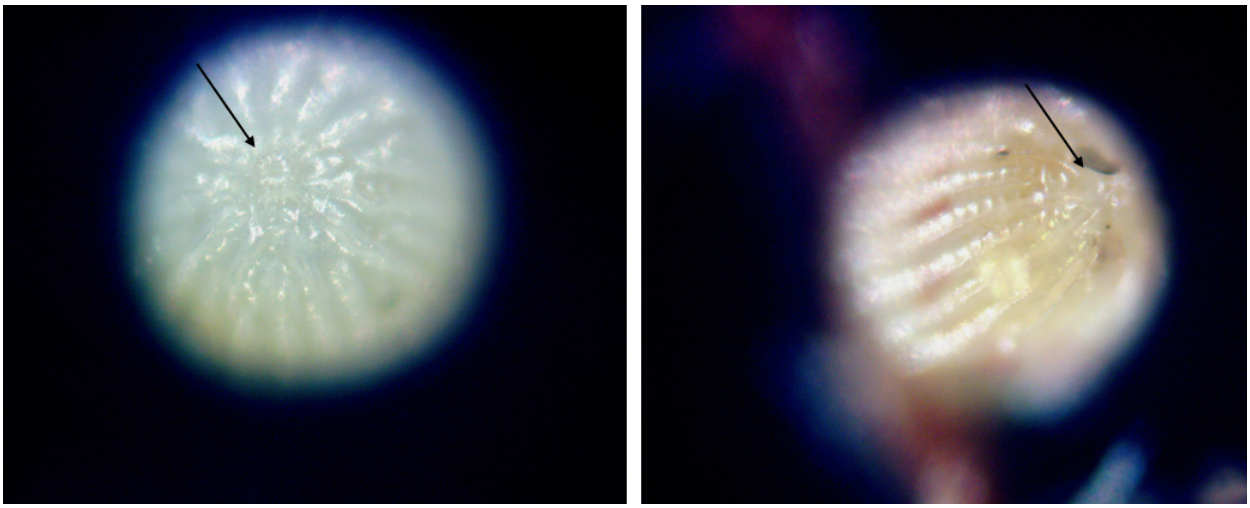

Figure 12. *Helicoverpa zea* eggs, (10X objective lens) photographs taken with a compound light microscope and AmScope attachment. Photo to the left is focused directly on the rosette area of the egg. Photo to the right is focused on the rosette area from an angle. Black arrows indicate the location of expected diagnostic morphological features (primary ribs extending to rosette and cross-ribs present).

Using a compound light microscope and an AmScope camera attachment, the micropyle region of both egg species were photographed to visualize the morphological differences between species. Two different angles were photographed in order to assess how difficult it would be to visualize morphological differences when not focused directly on the micropyle region. For *C. virescens*, the "gap" present between the primary ribs and the rosette was visible, but the other morphological differences (absence of cross-ribs) were difficult to see (Fig. 11). Additionally, when photographed at an angle, the "gap" was more difficult to see in comparison to when focused directly on the rosette (Fig. 11). For *H. zea*, the primary ribs extending to the rosette were visible, but the other morphological differences (presence of cross-ribs) were difficult to see (Fig. 12). Additionally, when photographed at an angle, the primary ribs extending to the rosette were difficult to see in comparison to focusing directly on the rosette (Fig. 12).

Figure 13. *Chloridea virescens* egg photographs (20X) taken with a Canon 60D DSLR and 20X microscope lens attachment. Two different eggs are pictured left and right. Black arrows indicate the location of expected diagnostic morphological features (primary ribs not extending to rosette and cross-ribs absent).

Figure 14. *Helicoverpa zea* egg photographs (20X) taken with a Canon 60D DSLR and 20X microscope lens attachment. Two different eggs are pictured left and right. Black arrows indicate the location of expected diagnostic morphological features (primary ribs extending to rosette and cross-ribs present).

The second photographic method examined used a Canon 60D DSLR camera with a 20X microscope lens attachment. For *C. virescens*, the diagnostic morphological characteristics were clear. There was a "gap" present where the primary ribs do not extend to the rosette and cross-ribs were absent (Fig. 13). For *H. zea*, the diagnostic morphological characteristics were also clear. The primary ribs extended to the rosette and cross-ribs were visible (Fig. 14).

For both of these photography approaches, different aged frozen eggs were used. Frozen eggs (Figs. 11-14) had to be used because of challenges with colony collapse due to COVID19 and reduced access to labs for colony maintenance. The differences in shape and color seen in the photographs are due to age differences and freezing. For this reason, color and shape were not considered during the analysis of photos. In future, eggs will be photographed immediately after oviposition to prevent this issue as well as other morphological differences that occur as the egg matures. Due to this experimental flaw, we focused only on two major morphological differences, the "gap" present in *virescens* and presence of cross-ribs in *zea*. Additionally, these two diagnostic morphological characteristics are the easiest to visualize and are also unaffected by freezing. While the morphological differences are visible using the light microscope and camera attachment, the highest quality photos were taken using a portable Canon 60D DSLR camera with a 20X lens attachment (Fig. 14). It is possible that using similar equipment and with little training, growers and/or scotts could examine and/or photograph eggs in the field for species ID. Once photographed, an algorithm also could be developed to ID eggs. Currently there is an application, iNaturalist, that uses an algorithm and user-based identifications to identify photos of plants, animals, and insects (www.iNaturalist.org). Since this technology already exists, it would be simple to examine this approach to identify insect eggs in the field. The other area of interest is the use of cameras on cell phones.

Conclusions and Future Directions

In conclusion, we were able to determine that differences in the surface chemical components between *H. zea* and *C. virescens* exist. In the near future, we will be conducting experiments further characterizing the surface chemical components of both species using Time of Flight Mass Spectrometry and GC-Mass Spectrometry. Once differences in surface components can be established, this will suggest that differential staining might be used for a field kit for species diagnosis. In regards to UV fluorescence and differences in color between egg species, we were unable to detect any fluorescence or differences in color with the eggs and wavelengths of light used for lab reared insects. In the future, these experiments should be repeated using field collected eggs and different wavelengths of UV-light. Lastly, we were successfully able to visualize the morphological differences between the two species. The best results were found using a portable camera with a microscope lens attachment. Of these photographs the "gap" present in *C. virescens* was the easiest to visualize. Once a database of species identified eggs showing these morphological differences can be established, egg species potentially could be quickly and effectively diagnosed in the field.

Acknowledgements

This work was funded by a grant from Cotton Inc. and supported by the NC Ag. Research Foundation. The authors would like to thank Grayson Cave of the NCSU Entomology and Plant Pathology department with his advice and assistance with insect colony maintenance. We would also like to thank Dr. Elaine Zhou of the NC State Analytical Instrumentation Facility and Dr. Matt Bertone of the NC State Entomology and Plant Pathology Department Plant Disease and Insect Clinic for their work with data collection.

References

Del Pozo-Valdivia, A. I., Reisig, D.D., Braswell, L., Greene, J.K., Roberts, P., and Taylor, S.V., In press**.** Economic injury levels for Bt-resistant Helicoverpa zea in cotton. J. Econ. Entomol. doi: 10.1093/jee/toab012

Environmental Protection Agency (EPA). Slowing and Combating Pest Resistance to Pesticides. Available online: https://www.epa.gov/pesticide-registration/slowing-and-combating-pest-resistance-pesticides. (Accessed 20 Oct 2020).

Greenstone, M.H., 1995. Bollworm or budworm? Squashblot immunoassay distinguishes eggs of Helicoverpa zea and Heliothis virescens (Lepidoptera: Noctuidae). J. Econ. Entomol. 88: 213-218.

Hagler, J.R., Cohen, A., Enriquez, F.J., and Dunlop, D.B., 1991. An egg-specific monoclonal antibody to Lygus hesperus. Biol. Cont. 1: 75-80.

Kumlert, R., Chaisiri, K., Anantatat, T., Stekolnikov, A.A., Morand, S., Prasartvit, A., Makepeace, B.L., Sungvornyothin, S., Paris, D.H., 2018. Autofluorescence microscopy for paired-matched morphological and molecular identification of individual chigger mites (Acari: Trombiculidae), the vectors of scrub typhus. PLOS ONE 13(3): e0193163. https://doi.org/10.1371/journal.pone.0193163

Lawrie, R.D., Mitchell, iii R.D., Deguenon, J.M., Ponnusamy, L., Reisig, D., Pozo-Valdivia, A.D., Kurtz, R.W., and Roe, R.M. 2020. Multiple Known Mechanisms and a Possible Role of an Enhanced Immune System in Bt-Resistance in a Field Population of the Bollworm, *Helicoverpa zea*: Differences in Gene Expression with RNAseq. *Int. J. Mol. Sci.* 21(18):E6528. doi: 10.3390/ijms21186528. PMID: 32906662.

Luttrell, R.G., Knighten, K., Kitten, W.F., Andrews, G.L., Harris, F.A., and Reed, J.. 1991. Monitoring pyrethroid resistance in the tobacco budworm in Mississippi: implications for resistance management. Agris. 15: 5-26.

Plapp, F.W., Jackman, J.A., Campanhola, C., Frisbie, R.E., Graves, J.B., Luttrell, R.G., Kitten, W.F., and Wall, M.. 1990. Monitoring and management of pyrethroid resistance in the tobacco budworm (Lepidoptera: Noctuidae) in Texas, Mississippi, Louisiana, Arkansas, and Oklahoma. J. Econ. Entomol. 83:335-341.

Reisig, D., Kerns, D., Gore, J., and Musser, F., 2019**.** Managing pyrethroid- and Bt-resistant bollworm in southern U.S. cotton. Crops & Soils. 52: 30-35

Trowell, S.C., Lang, G.A., and Garsia, K.A., 1993. A Heliothis identification kit. In S. Corey, D. Dall, and W. Milne [eds.], Pest control and sustainable agriculture. CSIRO, Melbourne, Australia. Pp. 174-177.

University of California. University of California Agriculture and Natural Resources: UC Pest Management Guidelines for Corn Earworm in Corn. Available online: http://ipm.ucanr.edu/PMG/r113300911.html (Accessed 20 Oct 2020). A

University of California. University of California Agriculture and Natural Resources: UC Pest Management Guidelines for Tobacco Budworm in Cotton. Available online: http://ipm.ucanr.edu/PMG/r114300611.html (Accessed 20 Oct 2020). B

University of Florida. University of Florida Entomology and Nematology Department. Available online : http://entnemdept.ufl.edu/creatures/field/tobacco_budworm.htm. (Accessed 19 Oct 2020).

USDA. *Pests and Diseases of Cotton*; United States Department of Agriculture: Washington, DC, USA, 1925.

Zeng, F., Ramaswamy, S.B., and Pruett S., 1998. Monoclonal Antibodies Specific to Tobacco Budworm and Bollworm Eggs. Journal of Physiology, Biochemistry, and Toxicology. 91: 677-684.